ELSEVIER

Biochimica et Biophysica Acta 1281 (1996) 91–100

BBA Biochimica et Biophysica Acta

Structural organisation and lipid composition of the epicuticular accessory layer of infective larvae of *Trichinella spiralis*

Kleoniki Gounaris *, Vincent P. Smith, Murray E. Selkirk

Department of Biochemistry, Imperial College of Science, Technology and Medicine, London SW7 2AY, UK

Received 28 November 1995; revised 12 January 1996; accepted 19 January 1996

Abstract

The epicuticle of infective larvae of *Trichinella spiralis* represents the interface between this intracellular nematode parasite and the cytosol of mammalian skeletal muscle. The macromolecular structures that make up the epicuticle were studied by freeze-fracture electron microscopy and compositional analysis. Three fracture planes were observed: one with a typical plasma membrane-type bilayer organisation which was overlaid by two extended layers of lipid in an inverted cylindrical configuration. This overall structure remained unchanged in response to variations in temperature between 20°C and 45°C. The lipid cylinders were on average 6.8 nm in diameter, with randomly-associated particles that were not dissociated by high-salt treatment, indicative of hydrophobically associated proteins. The majority of the lipids were non-polar, consisting of cholesterol, cholesterol esters, mono- and tri-glycerides, and free fatty acids. Three major classes of phospholipids were identified: phosphatidylethanolamine, phosphatidylglycerol and phosphatidylcholine. Total lipid extracts did not adopt an inverted cylindrical or micellar configuration on isolation, but formed flat sheets of lamellae as did the purified polar and non-polar fractions of the lipids. Isolated lipids did not undergo thermally-induced polymorphism between 20°C and 60°C and there was no pH dependency of the structures adopted. The fatty acid saturation levels of the phospholipids were compatible with the observation that they did not form polymorphic structures on isolation. We suggest that this unusual configuration is probably stabilised by the associated (glyco)proteins and may be required for selective permeation of nutrients from the host cell cytosol and/or for maintaining the high curvature of the parasite within the cell.

Keywords: Nematode; Cuticle; Freeze-fracture; Non-bilayer structure; Hexagonal II phase; (*T. spiralis*)

1. Introduction

The exoskeleton of all nematodes is the cuticle, an extracellular matrix composed primarily of collagen and a highly cross-linked outer cortex whose constituent proteins have been collectively termed cuticlin [1–5]. The cuticle is repeatedly shed and replaced during the life cycle as the organisms make the transition between one adult and four larval stages in a series of successive moults [1,2]. The cuticular matrix is bounded by a structure termed the epicuticle. The application of freeze-fracture electron microscopy to several nematode species has revealed fracture planes within the epicuticle consistent with the presence of membranes, although in some cases they displayed very few or no intramembranous particles characteristic of intrinsically associated proteins [6–9]. Although there is considerable variation between species and within different stages of the life cycle of the same species, studies in which fluorescent fatty acid analogues were incorporated into the surface of nematodes have yielded unusual results. Thus, a limited range of lipid probes appear to be able to insert into the epicuticle, and fluorescence recovery after photobleaching measurements have in general suggested that the structure is relatively immobile [10].

The infective larvae of *Trichinella spiralis* are highly unusual in that they invade skeletal muscle cells of their mammalian hosts and develop within the cytosol. These cells are transformed morphologically and metabolically into what is termed the 'nurse cell' [11]. Early on in this phase of development an electron-dense 'accessory layer' forms, which envelops the larva on the exterior face of the epicuticle. This accessory layer, which has been estimated to be about 15 nm thick, appears to remain in place until the entire cuticle is lost at the following moult which takes

Abbreviations: TLC, thin-layer chromatography; GC, gas-liquid chromatography; H_{II}, hexagonal type II lipid arrangement.

* Corresponding author. Fax: +44 171 5945207; e-mail: k.gounaris@ic.ac.uk.

PII S0005-2736(96)00022-3

place in the intestine of the subsequent host that ingests infected muscle [12,13]. Removal of the accessory layer in vitro by bile and trypsin results in a greatly enhanced rate of transcuticular uptake of glucose and concominantly, larval behaviour changes from coiling/uncoiling to sinusoidal movement [14]. Insertion of fluorescent lipid probes into adult and infective stage parasites indicated that the properties of the surfaces were different since both a C-18 fatty acid (5-(*N*-octadecyl)aminofluorescein) and a cholesterol analogue (nitrobenzoxadiazolamine-cholesterol) were inserted in adult but not in infective stage parasites [10].

Freeze-fracture studies of the surface accessory layer of infective larvae have been performed [15,16], and it was noted that the ultrastructure of the larvae is unusual. Two related models have been proposed to account for the morphology of the accessory layer. One proposes that it is made up of two layers, the outermost of which contains globules enveloped in a matrix while the inner layer consists of filaments [15]. In the second model it was proposed that the accessory layer consists of an outer layer of globular proteins which is associated with phosphatidylethanolamine tubular micelles [16].

In this study we examined the structural organisation and lipid composition of the accessory layer of muscle stage larvae of *T. spiralis*, and show that it is extremely unusual in that it is composed of two sheets of lipid in an inverted cylindrical configuration which overlay a membrane with a more conventional bilayer organisation. The surface lipids do not adopt the non-bilayer structural arrangements on isolation, and we found no conditions under which lipid polymorphism could be induced in vitro. These findings lead us to believe that specific interactions between the lipid and (glyco)protein components of the parasite's surface are required to stabilise the conformational arrangement of the accessory layer of the infective larvae.

2. Materials and methods

2.1. Parasites

Muscle stage infective larvae of *Trichinella spiralis* were isolated from outbred mice two months following infection. Minced mouse carcasses were digested in 1% pepsin, 1% HCl for 1.5 h at 37°C. Parasites recovered in a Baermann apparatus were washed extensively in phosphate-buffered saline, pH 7.4 (PBS), prior to preparation for electron microscopy, surface labelling or lipid extraction. Diaphragms from infected mice were also minced with scissors and prepared for freeze-fracture electron microscopy.

2.2. Extrinsic iodination and lipid extraction

Parasites were labelled with Iodogen as previously described [17] using 200 μg of Iodogen (Pierce Chemicals) and 250–500 μCi of $Na^{125}I$ (Amersham IMS 30) in PBS. Labelled worms were washed three times in PBS prior to lipid extraction.

Labelled or unlabelled parasites were treated according to the method described in [18] and the extracted lipid recovered, dried under a stream of nitrogen and resuspended in a small volume of chloroform/methanol (2:1, v/v). Lipid samples were used for freeze-fracture electron microscopy, thin-layer chromatography or fatty acid analyses and were treated as described in the following sections.

2.3. Thin-layer chromatography (TLC)

Extracted lipids were chromatographed on silica gel 60 (Merck) plates. TLC plates were developed in chloroform/methanol (1:1, v/v) and heated at 110°C for 30 min prior to use. Separation of the non-polar from the polar lipid classes was achieved by using hexane/diethyl ether/formic acid (80:20:2, v/v). Separation of individual polar lipid classes was performed by chromatography in chloroform/methanol/water (65:25:4, v/v). Two-dimensional TLC was carried out by employing chloroform/methanol/water (65:25:4, v/v) in the first dimension and chloroform/methanol/acetic acid/ water (25:15:4:2, v/v) in the second dimension. Lipid standards were run on plates at the same time for all chromatography steps. Lipids were visualised either by autoradiography or by spraying the plates with 0.1% Rhodamine B in ethanol.

2.4. Fatty acid analyses

Lipid samples were transesterified using 1% H_2SO_4 in methanol [19]. Decaheptanoic acid (17:0) was used as a standard for quantitative analyses. A Perkin Elmer 8700 gas chromatograph was used for estimation of fatty acid methyl esters. Methylated fatty acid samples were finally dried under nitrogen and redissolved in hexane. Samples were injected onto a 15% DEGS on Chromosorb W.AW (100/120 mesh) column and subjected to the following thermal gradient: the column was kept at 150°C for 2 min after injection of the sample, brought up to 170°C at a rate of 3 C°/min, kept at 170°C for 10 min and then brought up to 190°C at a rate of 10 C°/min. Elution of fatty acid methyl esters was completed in about one hour under these conditions. Nitrogen was used as the carrier gas at a flow rate of 80 ml min^{-1} and at a pressure of 620 kPa. The injector and flame ionisation detector were maintained at 200°C and 250°C, respectively. The amounts of material in the chromatographic peaks were estimated by electronic digital integration of the amplified signal from the detector.

2.5. Freeze-fracture electron microscopy

Muscle stage parasites isolated as above were infiltrated with a solution of 30% glycerol in PBS (pH 7.4). The

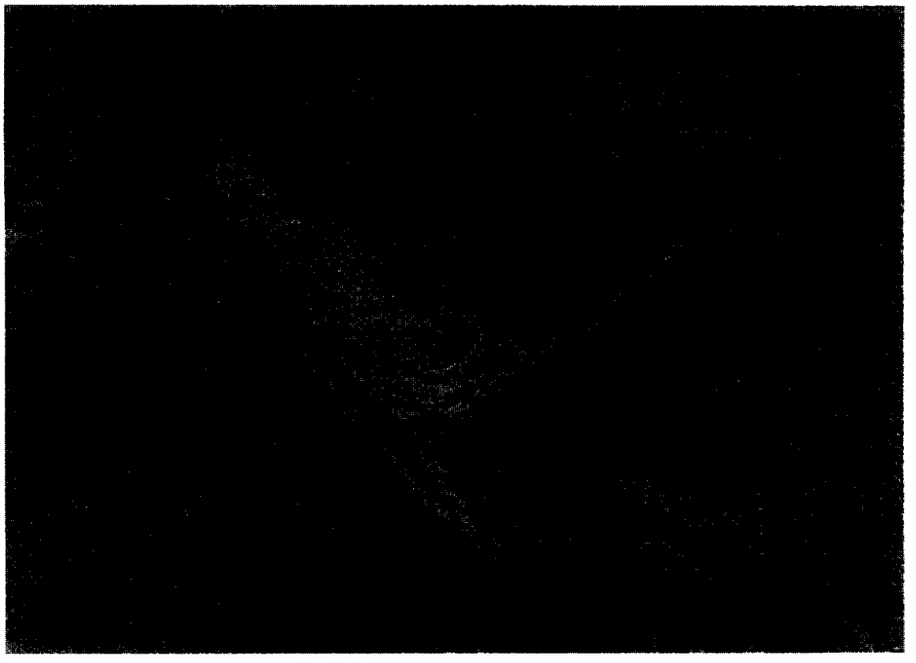

Fig. 1. Typical electron micrograph of freeze-fracture replicas obtained from *T. spiralis* muscle stage larvae demonstrating the presence of three fracture planes. Planes 1 and 2 represent the distal non-bilayer phases while in the proximal plane 3 the presence of a bilayer phase is shown. The arrow indicates the direction of shadowing and the bar is equal to 100 nm.

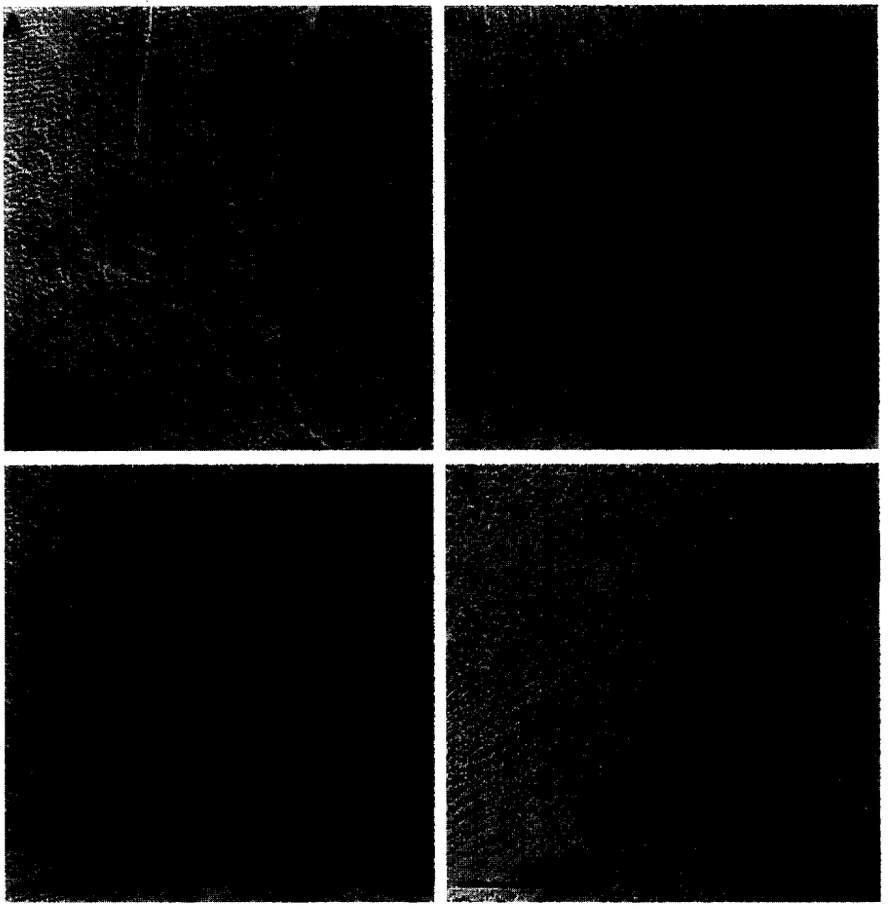

Fig. 2. Electron micrographs of freeze-fracture replicas of *T. spiralis* muscle stage larvae showing characteristic features of the accessory layer as discussed in the text. Arrows indicate the direction of shadowing and the bars are equal to 100 nm except in (D) where it is equal to 50 nm.

samples were thermally quenched from 37°C using a slurry of liquid and solid N_2 and fractured at −115°C in a Polaron freeze-fracture apparatus. Replicas, prepared by shadowing with platinum and carbon, were cleaned by treatment with bleach. Fracturing of infected diaphragms was also carried out as above. Lipid extracts in chloroform/methanol (1:1, v/v) were dried under a stream of N_2 and resuspended in either PBS (pH 7.4) containing 30% glycerol, or 20 mM solutions containing 30% glycerol and buffered at different pH values (20 mM Mes, pH 5.0; 20 mM BisTris propane, pH 7.0 and pH 9.0). All solutions were saturated with nitrogen. The lipid extracts were dispersed by ultrasonic irradiation prior to fracturing. Samples were thermally quenched from various temperatures as indicated, fractured and shadowed as described above. The replicas were cleaned in chloroform/methanol (1:1, v/v). All samples were examined using a Philips EM 301G electron microscope at 100 kV.

3. Results

We first examined the structural organisation of the epicuticle of *T. spiralis* muscle stage larvae by freeze-fracture electron microscopy on isolated parasites. A typical electron micrograph is shown in Fig. 1. We observed three fracture planes; the two most distal fracture planes (denoted as 1 and 2) indicated a non bilayer cylindrical configuration of the lipid components reminiscent of the hexagonal type II (H_{II}) organisation. The proximal fracture

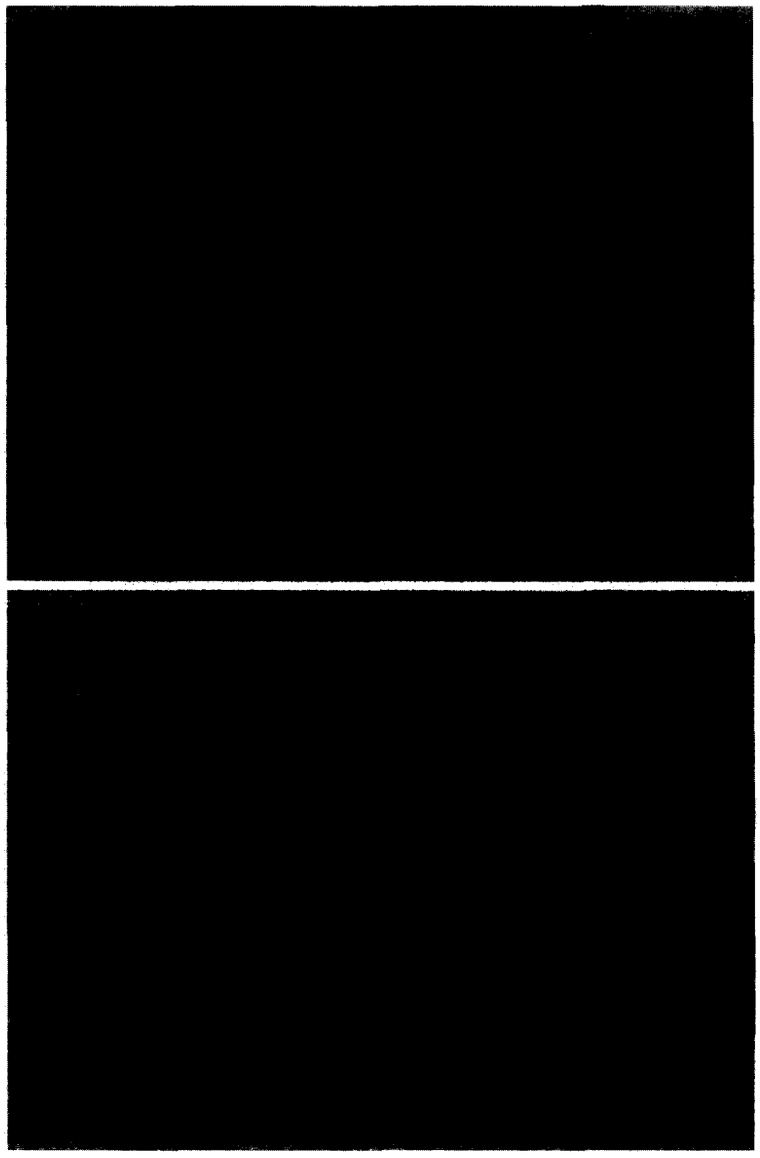

Fig. 3. Electron micrographs of freeze-fracture replicas obtained from diaphragm segments from a rat infected with *T. spiralis*. The asterisk in (A) indicates the presence of non-bilayer arrangements in situ. Arrows indicate the direction of shadowing and the bars are equal to 100 nm.

plane was of a conventional bilayer configuration (denoted as 3) and a significant number of randomly distributed particles were associated with the lipid structures. Measurements on a large number of replicas gave an estimated average diameter of the lipid cylinders of 6.8 nm. We also estimated the distance between the two non-bilayer planes to be about 7–8 nm, while the overall distance from the most distal non-bilayer plane 1 to the bilayer plane 3 was estimated to range between 16 and 20 nm.

In Fig. 2 some features of the freeze-fracture replicas are indicated. Distortions on the cylindrical structure were occasionally observed (Fig. 2A) which in general appeared as rows of globular micelles. Curvature of the lipid cylinders was a common feature in some of the replicas (Fig. 2B). In the majority of cases the two layers of the cylinders appeared to be parallel to each other as expected, but occasionally a lack of register was evident (Fig. 2B). We have no explanation for this observation other than it could be due to distortions in one of the layers that gives rise to the apparent curvature of the cylinders. A large number of randomly distributed particles were associated with the cylinders (Fig. 2C) which appeared to be strongly interacting with the lipid component, as repetition of the freeze-fracture procedure on parasites washed with 1 M NaCl, $CaCl_2$ or $MgCl_2$ resulted in replicas displaying indistinguishable morphology (data not shown). The particles associated with the bilayer fracture plane were approximately twice the diameter of those associated with the cylindrical structures. Fracture planes going across both non-bilayer stuctures down to the bilayer plane were commonly observed (Fig. 2D).

We thermally quenched larval samples at different temperatures ranging between 20°C and 45°C in order to examine whether the appearance of the non-bilayer configuration was temperature dependent. Freeze-fracture replicas of samples quenched at all temperatures tested were indistinguishable from those quenched at 37°C (data not shown). We considered the possibility that the appearance of the non-bilayer arrangement of the lipid molecules was an artefact of the procedure involved in the isolation of

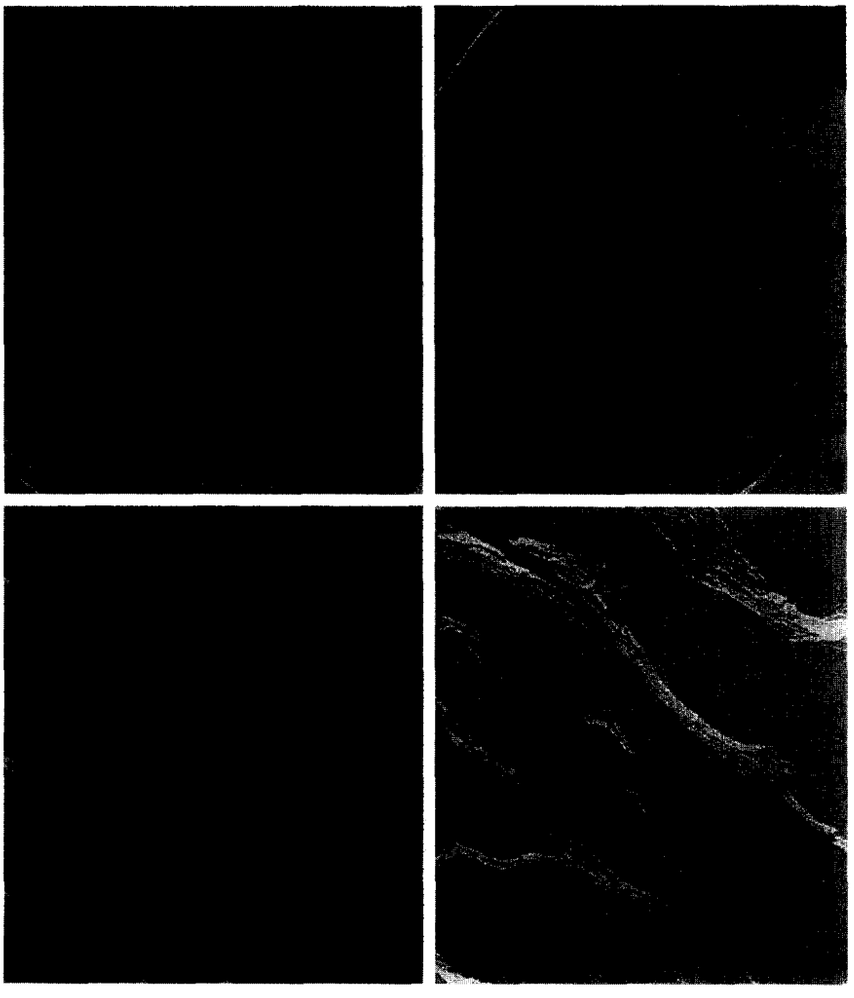

Fig. 4. Typical freeze-fracture electron micrographs obtained from replicas of aqueous dispersions of epicuticular *T. spiralis* lipids. (A) Total lipid extract, quenched from 60°C; (B) polar lipid fraction; (C) non-polar lipid fraction; (D) total lipid extract resuspended in buffer at pH 9.0. The direction of shadowing is indicated by the arrows and the bars represent 100 nm.

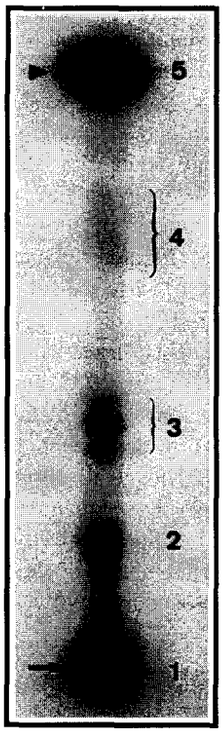

Fig. 5. Autoradiography of one dimensional thin-layer chromatograph of surface iodinated lipid extracts from *T. spiralis* resolving the non-polar lipid fraction as discussed in the text. The arrow indicates the origin and the arrowhead the solvent front. Identification of the lipid classes is as follows: (1) total polar lipids; (2) cholesterol; (3) free fatty acids; (4) triglycerides; (5) cholesterol esters.

parasites. Segments of diaphragm from a rat infected with *T. spiralis* were therefore directly subjected to freeze-fracture analysis. Fig. 3A illustrates a cross fracture of a parasite in a muscle cell. Longitudinal fracture planes along the parasite surface were extremely difficult to find, but as can be seen in higher magnification in Fig. 3B, the existence of the non-bilayer cylinders is apparent in the epicuticle in situ, indicating that this is the normal organisation of the lipid component in vivo.

To examine whether the epicuticular lipid formed non-bilayer structures on isolation, we extracted the lipid components and performed freeze-fracture electron microscopy on the isolated lipid samples. We observed that the lipids on isolation adopted neither a non-bilayer configuration nor a more conventional organisation of bilayers in liposomes. Instead, flat sheets of lamellae were observed as seen in Fig. 4. The lipid samples were also thermally quenched at different temperatures (10°C, 20°C, 30°C, 40°C and 60°C) prior to freeze-fracture, but all the replicas displayed an indistinguishable configuration of flat sheets of lamellae. Fig. 4A shows a typical replica of a lipid extract sample quenched from 60°C. Considering that the majority of the lipid was found to be non-polar (see Fig. 5), we further separated and purified by thin-layer chromatography the non-polar and the polar fractions of the lipid extract and examined both by freeze-fracture electron microscopy. Again flat sheets of lamellae were observed to form independent of the nature of the lipid fraction (Fig. 4B, 4C). Variations in the pH of the suspending medium

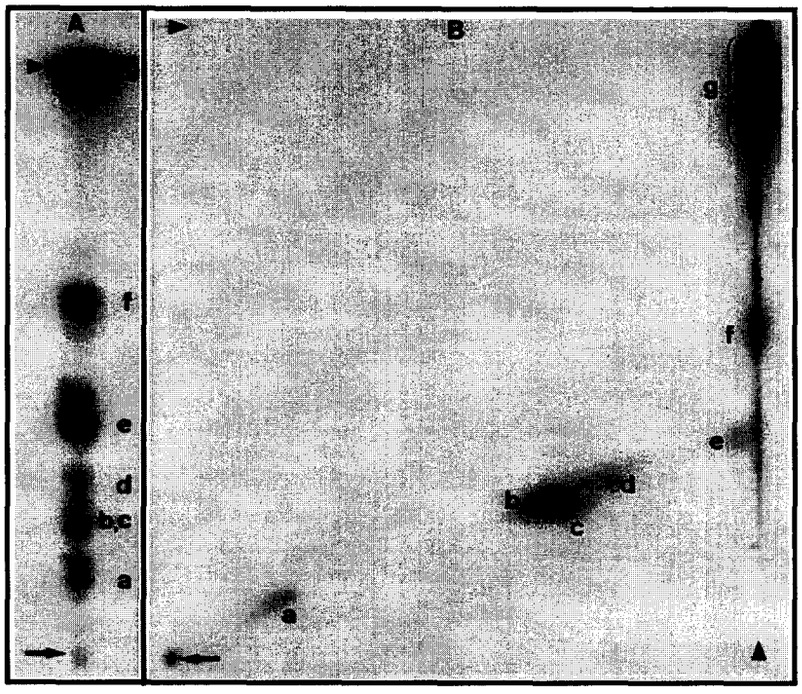

Fig. 6. Autoradiography of (A) one-dimensional and (B) two-dimensional thin-layer chromatographs resolving the polar lipid fraction of surface iodinated *T. spiralis* lipids. In each case the origin is indicated by an arrow and the solvent front by an arrowhead. Identification of the lipid classes is as follows: (a) lysophosphatidylcholine; (b) phosphatidylcholine; (c) lysophosphatidylethanolamine; (d) phosphatidylserine; (e) phosphatidylglycerol; (f) phosphatidylethanolamine; (g) total non-polar lipids.

Table 1
Fatty acid compositions of *T. spiralis* surface total lipids and surface-localised phosphatidylethanolamine

Fatty acid	Total surface lipid [a]	Surface PE [b]
12:0	0.29±0.08	0.20
14:0	1.58±0.04	1.35
14:1	0.25±0.03	none detected
16:0	7.51±0.15	7.96
16:1	0.30±0.05	0.38
18:0	28.88±0.08	26.89
18:1	13.95±0.09	12.28
18:2	3.52±0.16	2.96
18:3($n-6$)	0.24±0.03	0.05
18:3($n-3$)/20:0	0.97±0.19	1.26
20:2	1.10±0.04	1.14
20:3($n-6$)	1.19±0.11	1.13
20:3($n-3$)/20:4($n-6$)/22:0	22.10±0.09	18.14
24:0	15.80±0.18	24.49
22:6	2.32±0.06	1.74

[a] Fatty acid compositions are expressed as mean percentage weight ± standard deviation. Lipid classes from at least four separate groups of larvae were analysed.
[b] The fatty acid composition shown (percentage weight) is the average of two independent extractions. Errors were within ±0.5%.

had no discernible effect upon the structures adopted. Similar structures were observed at pH 5.0, 7.0 and 9.0, and a typical electron micrograph of a replica of a sample resuspended in buffer at pH 9.0 is shown in Fig. 4D. Thus, although the lipids adopt H_{II} configuration in the parasite epicuticle, they do not do so on isolation.

We next examined the composition of the epicuticular lipids by thin-layer chromatography (TLC) following extrinsic iodination of live parasites with Iodogen, a technique that has previously been demonstrated to specifically label surface components of nematodes [20]. Fig. 5 illustrates that non-polar lipids were a major constituent of the total lipid extract and could be identified as cholesterol esters, free fatty acids, mono- and tri-glycerides and cholesterol. Analyses of the polar lipid fraction by one-dimensional TLC (Fig. 6A) indicated a relatively simple composition, with the major classes identified as phosphatidylethanolamine, phosphatidylglycerol and phosphatidylcholine. Small amounts of lysophosphatidylethanolamine and lysophosphatidylcholine were also found in the majority of the extracts. We carried out two-dimensional TLC in order to further clarify the polar lipid composition, but no additional lipid classes were identified by chromatography in the second dimension (Fig. 6B).

The fatty acid composition of extracted lipids was determined by gas-liquid chromatography (GC), and the results are illustrated in Table 1. The fatty acids ranged in length from 12 to 24 carbon atoms. The most abundant fatty acid type was 18 carbons long which comprised approximately half of the total. The majority of the fatty acids were mainly saturated or monounsaturated and the overall unsaturation index was estimated at 0.499. We further tested the fatty acid composition of purified phosphatidylethanolamine since it is the only phospholipid present which could normally give rise to non-bilayer structures. As seen in Table 1 the fatty acid composition of this lipid class was very similar to that of the total surface lipid with an overall unsaturation index of 0.437. Since the method used for gas chromatography does not differentiate either between 20:3($n-3$), 20:4($n-6$) and 22:0 or 18:3($n-3$) and 20:0 we recalculated the unsaturation index assuming that all fatty acids at these positions were either 20:4($n-6$) or 18:3($n-3$). Even with this assumption the unsaturation indices for the total lipid and for phosphatidylethanolamine were calculated at 1.29 and 1.07, respectively. The saturation levels were thus incompatible with the isolated lipids forming non-bilayer structures, as indeed was demonstrated by the freeze-fracture replicas shown in Fig. 4.

4. Discussion

The data obtained indicate that the accessory layer of the epicuticle of muscle stage larvae of *Trichinella spiralis* is composed of two extensive sheets of lipid in a non-bilayer configuration which overlay a conventional lipid bilayer (Figs. 1 and 2). The non-bilayer configuration appears to be of the hexagonal type II (H_{II}) arrangement with an estimated average diameter of the cylinders of 6.8 nm. This is not an artefact of the procedure used to isolate parasites, as freeze-fracture electron microscopy of larvae in situ in cells of the diaphragm of infected mice resulted in replicas with identical morphology (Fig. 3). Although we cannot establish from the experiments reported here that the entire surface of the larva is covered with these structures, we have not been able to obtain evidence to the contrary and data from morphological studies suggests that this may well be the case [15].

Freeze-fracture particles appeared in association with both the H_{II} layer and the underlying bilayer, but are particularly densely distributed on the former structures (Figs. 1 and 2). As the appearance of the replicas did not change after washing larvae with high salt concentrations, we consider that these particles do not represent proteins non-specifically associated with the organism or attached via electrostatic interactions but rather represent (glyco)proteins which are associated with the parasite surface via hydrophobic interactions.

The lipid composition of the surface of the parasite appeared to be enriched in neutral lipids and the polar lipid fraction had a simple class composition. Phosphatidylethanolamine, which potentially could give rise to non-bilayer configurations, does not appear to dominate the total lipid content and has a low unsaturation index. We therefore consider it unlikely that this lipid class is the sole contributor to the formation of the H_{II} cylinders [16]. In addition, neither the total lipid extract nor the separated

polar or neutral lipid fractions adopted the H_{II} configuration on isolation and we found no conditions of temperature or pH which could induce non-bilayer structures in the isolated lipids. The fatty acids of the lipids were mostly saturated or monounsaturated, consistent with the apparent lack of polymorphic phases. The diameter of the cylinders is larger than that reported for H_{II} cylinders formed by purified lipid classes in other systems (normally 4–5 nm) and is distinct from the dimensions estimated for binary lipid mixtures which give rise to cylindrical inverted micelles or cubic phases [21–23]. It is of interest that the isolated parasite lipids did not form liposomes in aqueous dispersions but assumed an extended flat lamellar arrangement. Similar structures have previously been reported for purified H_{II}-forming lipids which had been subjected to either catalytic hydrogenation or to low temperatures [24]. Extended lamellar sheets have also been reported to be formed by lipids of mammalian stratum corneum which are able to undergo thermotropic polymorphism [25]. We found no conditions however, within the temperature range tested, which could induce the H_{II} configuration in the isolated parasite lipids.

Membrane conformations other than a lipid bilayer are in general not considered to be adopted as stable configurations in biological systems. Non-bilayer arrangements have been reported to occur transiently during membrane fusion [26] or locally at tight junctions [27]. However, the formation of non-bilayer configurations in biological membrane systems in response to stress conditions such as elevated temperatures [28], freeze-induced dehydration [29] or ischaemia [30] invariably results in membrane destabilisation and irreversible damage to the system. The only two systems that have been suggested to consist of membrane networks arranged in structures resembling non-bilayer configurations are the prolamellar body of plant etioplasts [31,32] and the surface membrane of the thermophilic archaebacterium *Sulfolobus solfataricus* [33,34]. In the former case a highly ordered, branched tubular membrane organisation is observed similar to a bicontinous cubic phase and it has been suggested that the dominant protein complex in these structures, namely NADPH–protochlorophyllide oxidoreductase, induces or facilitates this organisation. In the case of *S. solfataricus* it has been proposed that a three dimensional network in the cubic phase could act to protect bacteria against fluctuations in temperature.

The extent of the stable non-bilayer H_{II} structures observed on the surface of this intracellular parasite is unprecedented in living organisms. Stable non-bilayer configurations are considered detrimental to the barrier properties of the membrane, and indeed a H_{II} configuration on the surface of the parasite would even be thermodynamically unfavourable. A possible overall arrangement that we envisage, which would be thermodynamically acceptable, is one in which the two H_{II} layers are overlaid by at least one monolayer of lipid on both sides. Implicitly, we would expect that the associated (glyco)proteins would traverse both the distal H_{II} cylinders and the outer monolayer. A schematic representation of the suggested lipid arrangement is presented in Fig. 7. This model implies the existence of four fracture faces indicated as A, B, C and D. Face A and face B would give rise to the cylindrical micellar appearance seen in Fig. 1 and indicated as planes 1 and 2. Face D could correspond to fracture plane 3 which implies the presence of a bilayer membrane with integral proteins beneath the cylindrical structures. Fracturing through face C, however, would be indistinguishable from face D, assuming that the monolayer directly below the cylinders contains proteins. In fact, our measurements for the overall distance between the most distal non-bilayer plane 1 to the bilayer plane 3 varied between 16 and 20 nm and the discrepancy in the values could be due to the fracture plane going either through face C or D. This of course would mean that what is referred to as plane 3 could be originating from either of the two fracture planes.

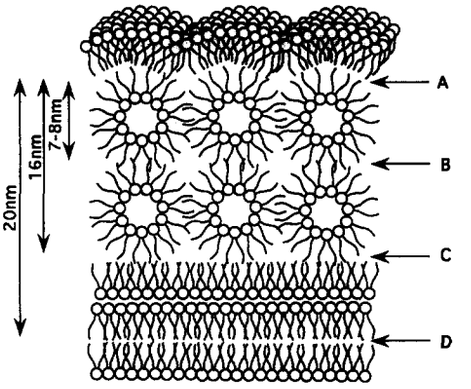

Fig. 7. Schematic representation of a possible overall arrangement of lipids in the epicuticular accessory layer of infective larvae of *Trichinella spiralis*. Four fracture faces are denoted as A, B, C and D and the estimated distances between these faces are indicated. Further explanations are presented in the text. The model is not drawn to scale, and the depiction of all lipids with two hydrophobic chain substituents as well as the number of molecules associated with each cylinder is arbitrary.

It is possible that the interaction of the associated (glyco)proteins with the lipid component is necessary for the induction of this non-bilayer arrangement, and this is currently under examination. It is known that a number of bioactive peptides, toxins and certain proteins influence the polymorphic behaviour of lipids [35–37]. The repertoire of surface proteins of infective larvae of *T. spiralis* has been defined by extrinsic iodination experiments and like all nematodes examined thus far, it presents an extremely restricted profile. Two basic glycoprotein subunits of 51 and 55 kDa form covalently-linked homodimers of 90 and 105 kDa, respectively when resolved by SDS-PAGE under reducing conditions [38]. The mode of anchorage of these glycoproteins to the surface of the parasite remains undetermined, but it is possible that they are responsible for stabilising this unusual lipid configuration.

Experiments previously reported on the ability of cer-

tain lipid probes to insert into the surface of the parasite, and on the mobility of these probes as judged by recovery of fluorescence after photobleaching [39] can be accounted for by both the apparent structural organisation of the parasite's surface and the low unsaturation index of the fatty acids. Thus, few probes would be expected to insert, and mobility within the lipid H_{II} cylinder would be highly restricted. Incubation of infective larvae in bile and trypsin in vitro resulted in the dissolution of the accessory layer, and was accompanied by a change in behaviour from coiling/uncoiling to sinusoidal movement, which the authors interpreted as consistent with progression to the next niche in the life cycle [14]. Incubation of larvae in bile and trypsin also results in enhanced insertion of previously restricted fatty acid probes into the surface of the parasite [40]. Loss of the accessory layer might remove restrictions imposed by the non-bilayer organisation, although it has been observed that the accessory layer is still intact by the time the larvae are established in the epithelium of the small intestine [12], and indeed may not be lost until the entire cuticle is shed at the following moult [13].

Although we can only speculate on the purpose of the extensive sheets of lipid in H_{II} configuration, it is presumably essential for survival of parasites in the muscle cell, as this is the only phase of the life cycle of the parasite in which it is evident, and the phenomenon has not been documented for any other nematode species. It might be possible that the accessory layer provides protection to the parasite during passage through the stomach of the subsequent host that ingests infected muscle. Parasites that had been depleted of this layer by treatment with high concentrations of detergent were killed by incubation in 1% pepsin/HCl at pH 1.5 [16], although it is difficult to draw conclusions from such harsh conditions. It is perhaps more pertinent to note that many nematodes migrate through the stomach of mammalian hosts, but no other species have been demonstrated to display such modifications in surface structure.

It seems more likely that the adoption of surface lipid in H_{II} configuration is necessary for existence within the mammalian muscle cell. Although the lipid components alone do not appear to adopt non-bilayer conformations they might be induced to do so in vivo by their interaction with other hydrophobic molecules, perhaps in a similar manner in which alkanes or hydrophobic peptides induce H_{II} configurations in phosphatidylcholine systems [41,42]. The permeability of such a macromolecular structure to solutes and other molecules would be significantly different to a conventional bilayer membrane and may facilitate the nutritional requirements of the larva. The high curvature of the parasite within the cell may be aided by the non-bilayer arrangement, and the resulting structure which restricts the parasite's movement is perhaps advantageous for its survival in the intracellular milieu.

Acknowledgements

We thank Dr. A.P.R. Brain for assistance with the freeze-fracture procedure. This work was supported by the Wellcome Trust. V.P. Smith is the recipient of a Wellcome Trust Prize Studentship (Ref. 038743/Z/93/Z/1.5E).

References

[1] Lee, D.L. and Atkinson, H.J. (1976) Physiology of Nematodes, 2nd Edn., Macmillan, London.
[2] Bird, A.F. (1980) in Nematodes as Biological Models (Zuckerman, B.M., ed.), Vol. 2, pp. 213–236, Academic Press, New York.
[3] Wright, K.A. (1987) J. Parasitol. 73, 1077–1083.
[4] Fujimoto, D. and Kanaya, S. (1973) Arch. Biochem. Biophys. 157, 1–6.
[5] Cox, G.N., Kusch, M. and Edgar, R.S. (1981) J. Cell. Biol. 90, 7–17.
[6] Martinez-Palomo, A. (1978) J. Parasitol. 64, 127–136.
[7] DeSouza, W., Souto-Padron, T., Dreyer, G. and Dias de Andrade, L. (1993) Exp. Parasitol. 76, 287–292.
[8] Peixoto, C.A. and DeSouza, W. (1993) Parasitol. Res. 80, 53–57.
[9] Lee, D.L., Wright, K.A. and Shivers, R.R. (1994) Parasitology 107, 545–552.
[10] Proudfoot, L., Kusel, J.R., Smith, H.V. and Kennedy, M.W. (1991) in Parasitic Nematodes-Antigens, Membranes and Genes (Kennedy, M.W., ed.) pp. 1–26, Taylor and Francis, London.
[11] Despommier, D.D. (1990) Parasitol. Today 6, 193–196.
[12] Wright, K.A. and Hong, H. (1989) Exp. Parasitol. 68, 105–107.
[13] Capo, V.A., Despommier, D.D. and Silberstein, D.S. (1984) J. Parasitol. 70, 992– 994.
[14] Stewart, G.L., Despommier, D.D., Burnham, J. and Raines, K.M. (1987) Exp. Parasitol. 63, 195–204.
[15] Lee, D.L., Wright, K.A. and Shivers, R.R. (1984) Tissue Cell 16, 819–828.
[16] Wright, K.A. and Hong, H. (1988) J. Parasitol. 74, 440–451.
[17] Maizels, R.M., Blaxter, M.L., Robertson, B.R. and Selkirk, M.E. (1991) Parasite Antigens, Parasite Genes: A Laboratory Manual for Molecular Parasitology, Cambridge, Cambridge University Press.
[18] Folch, J., Lees, M. and Sloane-Stanley, G.H. (1957) J. Biol. Chem. 226, 497–509.
[19] Christie, W.W. (1989) Gas Chromatography and Lipids: A Practical Guide, The Oily Press, Ayr, Scotland.
[20] Marshall, E. and Howells, R.E. (1985) Mol. Biochem. Parasitol. 15, 295–304.
[21] Quinn, P.J. and Williams, W.P. (1983) Biochim. Biophys. Acta 737, 233–266.
[22] Lindblom, G. and Rilfors, L. (1989) Biochim. Biophys. Acta 988, 221–256.
[23] Gounaris, K., Sen, A., Brain, A.P.R., Quinn, P.J. and Williams, W.P. (1983) Biochim. Biophys. Acta 728, 129–139.
[24] Gounaris, K., Mannock, D.A., Sen, A., Brain, A.P.R., Williams, W.P. and Quinn, P.J. (1983) Biochim. Biophys. Acta 732, 229–242.
[25] Abraham, W. and Downing, D.T. (1991) Biochim. Biophys. Acta 1068, 189–194.
[26] Verkleij, A.J. (1984) Biochim. Biophys. Acta 779, 43–63.
[27] Hein, M., Post, A. and Galla, H.J. (1992) Chem. Phys. Lipids 63, 213–221.
[28] Gounaris, K., Brain, A.P.R., Quinn, P.J. and Williams, W.P. (1984) Biochim. Biophys. Acta 766, 198–208.
[29] Webb, M.S., Hui, S.W. and Steponkus, P.L. (1993) Biochim. Biophys. Acta 1145, 93–104.

[30] Post, J.A., Bijvelt, J.J.M. and Verkleij, A.J. (1995) Am. J. Physiol. 268, 773–780.
[31] Ryberg, M., Sandelius, A.S. and Selstam, E. (1983) Physiol. Plant. 57, 555–560.
[32] Selstam, E. and Sandelius, A.S. (1984) Plant Physiol. 76, 1036–1040.
[33] Gulik, A., Luzzati, V., De Rosa, M. and Gambacorta, A. (1985) J. Mol. Biol. 182, 131–149.
[34] Gulik, A., Luzzati, V., De Rosa, M. and Gambacorta, A. (1988) J. Mol. Biol. 201, 429–435.
[35] Gasanov, S.E., Vernon, L.P. and Aripov, T.F. (1993) Arch. Biochem. Biphys. 301, 367–374.
[36] Epand, R.M., Epand, R.F., Richardson, C.D. and Yeagle, P.L. (1993) Biochim. Biophys. Acta 1152, 128–134.
[37] Streicher, S.J., Lapidus, R. and Sokolove, P.M. (1994) Arch. Biochem. Biophys. 315, 548–554.
[38] Parkhouse, R.M.E., Philipp, M. and Ogilvie, B.M. (1981) Parasite Immunol. 3, 339–352.
[39] Proudfoot, L., Kusel, J.R., Smith, H.V. and Kennedy, M.W. (1993) Parasitology 107, 559–566.
[40] Modha, J., Kusel, J.R. and Kennedy, M.W. (1995) Mol. Biochem. Parasitol. 72, 141–148.
[41] Lindblom, G., Sjölund, M. and Rilfors, L. (1988) Liq. Cryst. 3, 783–790.
[42] Sjölund, M., Rilfors, L. and Lindblom, G. (1989) Biochemistry 28, 1323–1329.